

Study of the Mechanisms of Initial Oxidation and of the Interaction with Reactive Elements in the Halogen Effect for Ni-base Alloys

H.-E. Zschau, B. Gleeson, M. Schütze
e-mail: zschau@dechema.de
Funded by: DFG
Period: 01.09.2014 – 31.08.2016



Introduction

Ni-base super alloys with Al-contents of less than 10 wt.-% are widely used in high temperature technology due to their beneficial mechanical properties (fig. 1). To achieve these properties the Al-content of such alloys is limited to a few % and thus they do not form a dense Al_2O_3 protective scale on the surface, but rather a complex layer structure as shown in fig. 2. The formed alumina scale is characterized by internal oxidation, i. e. it grows into the metal showing a discontinuous structure.



Fig. 1: The turbine blades for aircraft engines and gas fired power stations are manufactured with an Al-rich bond coat and a TBC.

Fig. 2: Oxide scale on IN738 after isothermal oxidation of 24h/1050°C/air.

In the manufacturing process the oxidation protection can be achieved by covering the Ni-base alloy with Al-rich coatings. An alternative method to form a protective alumina scale is proposed by using the halogen effect.

the 2 MV Van de Graaff - accelerator of the Institute of Nuclear Physics of the Goethe-University Frankfurt. To implant the same depth region in alloy IN 738 a F-ion energy of 38 keV was chosen in case of 110 keV Y-ions, whereas F-ions of 20 keV were used together with 100 keV Hf-ions. The implantation profiles strongly depend on the sequence of implanting Hf and F. If F was implanted first and followed by Hf (fig. 5) the calculated F-profile is slightly reduced compared to the single implantation case. Additionally the F-depth profile measured with PIGE reveals a distinct drop to values below 10 at.%. An internally growing non-protective alumina scale was formed after oxidation (fig. 4). The element maps in fig. 6 (obtained by EPMA) illustrate this.

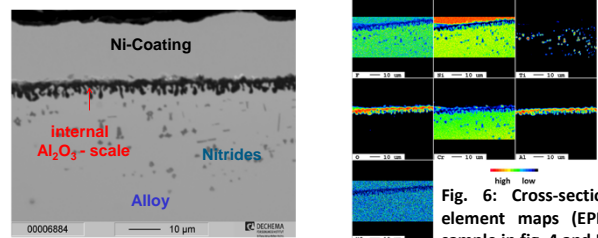


Fig. 6: Cross-section and element maps (EPMA) of sample in fig. 4 and 5.

First implantation of Hf and second of F changes the situation completely and makes the F-profiles reproducible. The measured F-profiles are in good agreement with the calculated profiles (fig. 7b,c). The calculated Hf-concentrations vary linearly within a region of

F-Effect for Ni-base Superalloys

The **halogen effect** „artificially“ increases the Al-amount on the surface forming a dense protective alumina scale. This concept - which works successfully in the case of TiAl-alloys - is now applied to Ni-base alloys. After doping the alloy surface with F and subsequent oxidation at 1050°C a change of the oxidation mechanism from an internally growing non-protective alumina scale into a dense continuous outer protective alumina scale is observed (fig. 3).

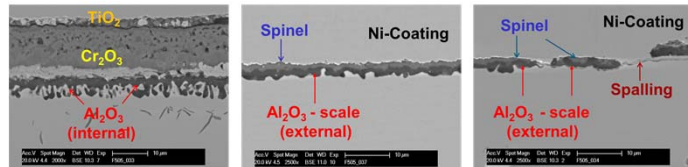


Fig.3: Left micrograph: Oxide scale on IN 738 (untreated) after oxidation (24h/1050°C/air). Middle micrograph: The implanted sample (7.5×10^{16} F cm⁻² /38 keV) shows after oxidation (60h/1050°C/air) the change from internal to external oxidation of Al, forming a protective scale. Right image: The formed protective alumina scale partly spalled during cooling (1×10^{17} F cm⁻² and 60h/1050°C).

The alumina scale formed by using the halogen effect protects the alloy IN 738 during isothermal oxidation up to at least 1000 h at temperatures of 1050°C. For cyclic oxidation the formed alumina scale partly spalls, obviously due to the mismatch in the coefficients of thermal expansion of the alumina scale and the Ni-base alloy.

Structure of Oxide Scale after F- and RE-Implantation

Small additions of reactive elements (Y, Hf, Ce...) are beneficial for the adhesion of protective alumina scales. Mostly RE are added as alloying elements. In this work a combined surface modification with fluorine and reactive elements was chosen. To find the optimum additions beam-line ion implantation was used because of its good accuracy and reproducibility. Additionally it is important to know if the implantation sequence plays a role. The implantations were planned by comprehensive Monte Carlo - calculations of the implantation profiles by using the T-DYN-software. All implantations were performed at the 60 kV-implanter, whereas the non-destructive analyses of F-, Hf- and Y-profiles were carried out by using the PIGE/RBS-techniques at

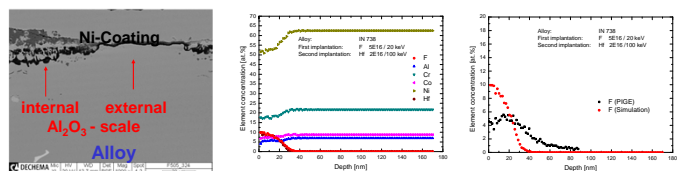


Fig. 4: Cross-section of alloy IN738 from fig. 5 after oxidation (85h/1050°C).

Fig. 5: Left: Element profiles (T-DYN-calc.) in IN 738 after implantation of F (5×10^{16} F cm⁻²/20 keV) and Hf (2×10^{16} Hf cm⁻²/ 100 keV). Right: Calc. and exp. (PIGE) F-profiles.

Fig. 7a, 7b, 7c: Left: Element profiles (T-DYN-calc.) in IN 738 after oxidation after implantation of Hf (2×10^{16} Hf cm⁻²/100 keV) and F (5×10^{16} F cm⁻²/20 keV). Right: Calc. and exp. (PIGE) F-profiles.

40 nm. An adherent protective alumina scale was found after oxidation (fig. 7a). The element mappings depicted in fig. 8 (measured by using EPMA) show a thin alumina scale, no nitrides are visible.

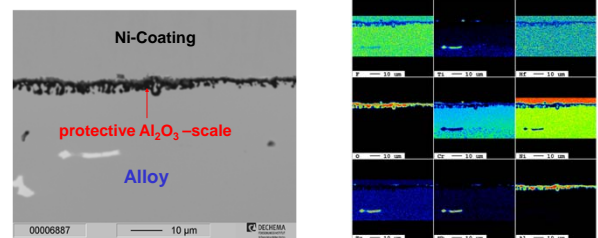


Fig. 8: Cross-section and element maps (EPMA) of sample in fig. 7 and 8.

Based on these results a screening by varying the Y- and F-fluences was performed achieving an adherent protective alumina scale for the parameters 4×10^{16} Y cm⁻² /110 keV and 5×10^{16} F cm⁻² /38 keV (fig. 9 - 10).

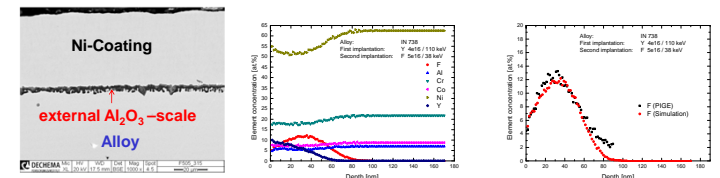


Fig. 9a: Cross-section of alloy IN738 after oxidation after implantation of Y (4×10^{16} Y cm⁻²/110 keV) and F (5×10^{16} F cm⁻²/38 keV). Right: Calc. and exp. (PIGE) F-profiles.

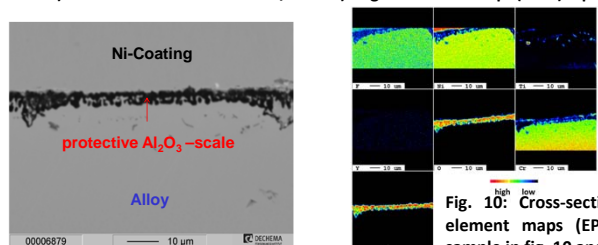


Fig. 10: Cross-section and element maps (EPMA) of sample in fig. 10 and 11.